

# **Imaging the Ionosphere Using Spaceborne Synthetic Aperture Radar**

Xiaoqing Pi

*Jet Propulsion Laboratory  
California Institute of Technology*

## Acknowledgment

Bruce Chapman (JPL), Anthony Freeman (JPL)  
Masanobu Shimada (JAXA), Franz Meyer (U. Alaska)  
Alaska Satellite Facility & International GNSS Service

Government Sponsorship Acknowledged

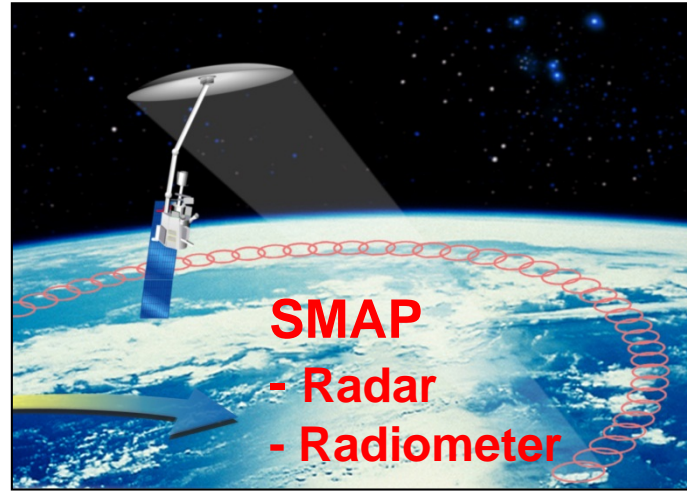
CEDAR Workshop, Santa Fe, NM, June 28, 2010



# Earth Science Radar Missions

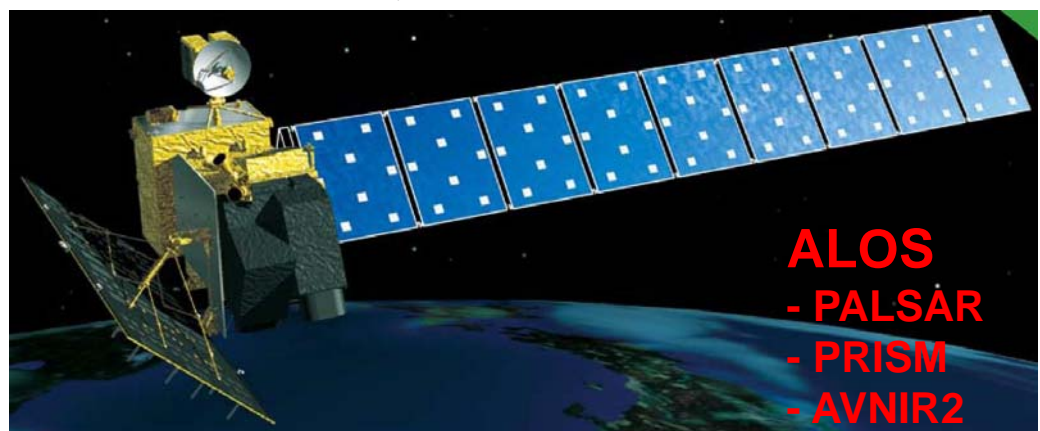


Global Sea Surface Salinity  
Launched in June 2011



Global Soil Moisture  
To be launched in 2015

**ALOS**  
Advanced Land Observing Satellite,  
JAXA's **InSAR** mission  
launched in Jan 2006.  
(ALOS-2 will follow.)



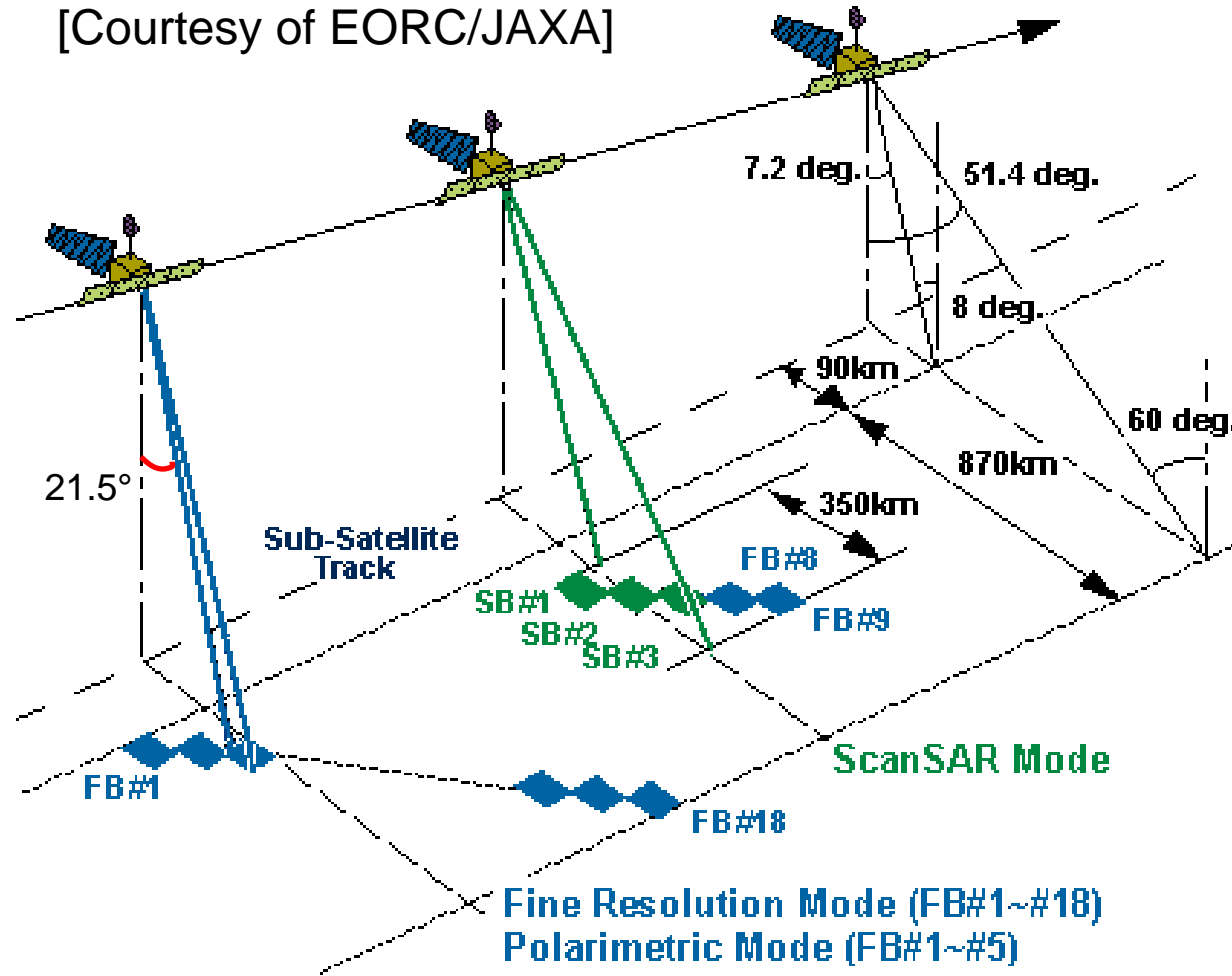
## DESDynI

Deformation, Ecosystem  
Structure, and Dynamics of Ice  
NASA **InSAR** Mission  
Under study



# Advanced Land Observing Satellite Phase Array type L-band SAR

[Courtesy of EORC/JAXA]



## ALOS (JAXA) Orbit

- ~690 km ALT
- $I = 98^\circ$  (Sun-synchronous 10 AM/10 PM)
- Repeat period: 46 days

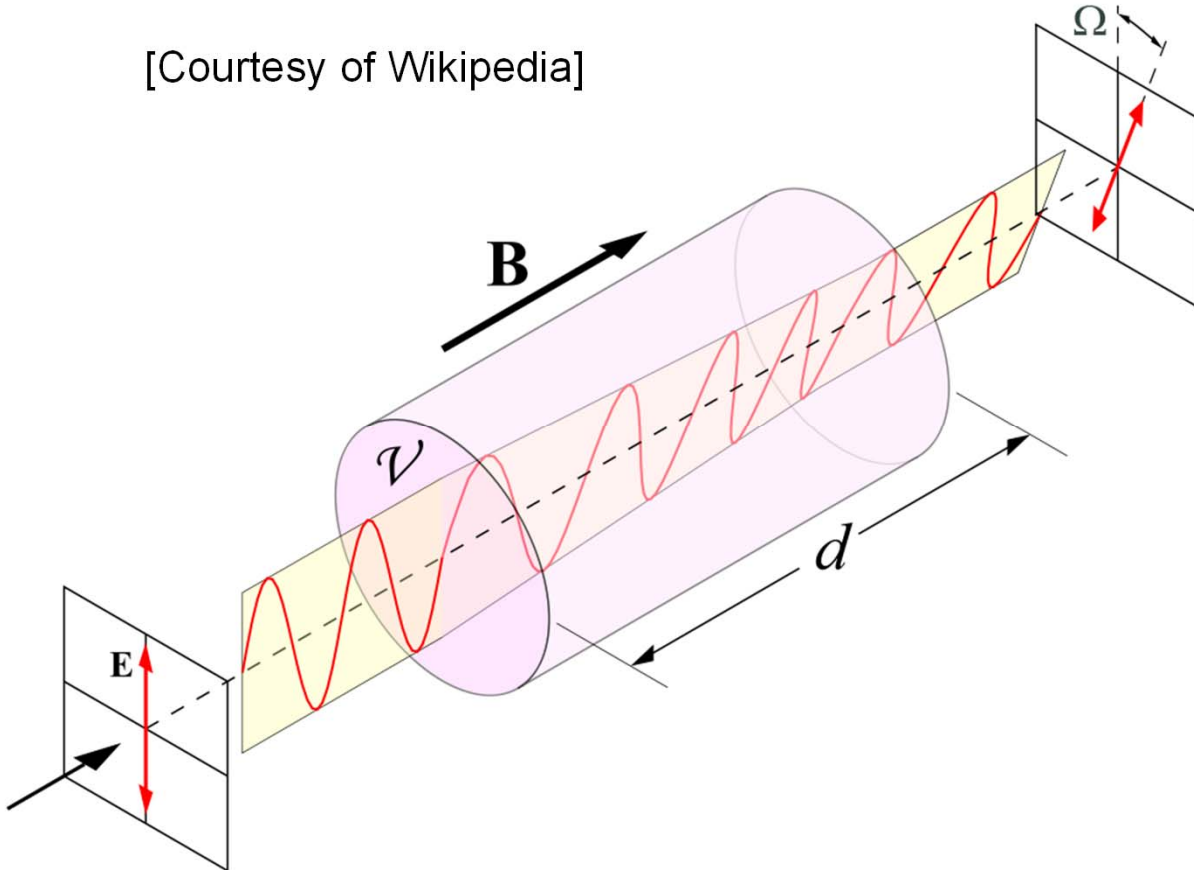
## PALSAR

- L-band: 1.27 GHz
- Signal chirp bandwidth: 28 MHz or 14 MHz for single-pol or multi-pol obs modes
- Experimental quad-pol mode among other observation modes (HH, HV, VH, and VV)
- Polarimetric image pixel spacings (resolutions)
  - Along track (azimuth) = 3.6 m
  - Cross track (range) = 9.4 m
  - Cross track (ground) = 23.3 m



# Faraday Rotation and TEC

[Courtesy of Wikipedia]



$$\Omega = \frac{K}{f^2} \int_{\mathbf{r}_t}^{\mathbf{r}_r} n_e B_0 \cos \theta ds$$

$$= \frac{K}{f^2} \langle B_0 \cos \theta \rangle \text{TEC}$$

$$\text{TEC} = \Omega \frac{f^2}{K \langle B_0 \cos \theta \rangle}$$

(for each radio link)

The effect is less sensitive near or at the magnetic equator for a nominal SAR system as  $\theta$  approaches  $90^\circ$  and  $\cos \theta$  becomes very small.



# Faraday Rotation Measurements Using PoISAR

---

- Polarimetric measurements (scattering matrix):

$$\begin{pmatrix} M_{hh} & M_{vh} \\ M_{hv} & M_{vv} \end{pmatrix} = A(r, \theta) e^{j\phi} \begin{pmatrix} 1 & \delta_2 \\ \delta_1 & 1 \end{pmatrix} \begin{pmatrix} 1 & 0 \\ 0 & f_1 \end{pmatrix} \begin{pmatrix} \cos \Omega & \sin \Omega \\ -\sin \Omega & \cos \Omega \end{pmatrix} \begin{pmatrix} S_{hh} & S_{vh} \\ S_{hv} & S_{vv} \end{pmatrix} \\ \cdot \begin{pmatrix} \cos \Omega & \sin \Omega \\ -\sin \Omega & \cos \Omega \end{pmatrix} \begin{pmatrix} 1 & 0 \\ 0 & f_2 \end{pmatrix} \begin{pmatrix} 1 & \delta_3 \\ \delta_4 & 1 \end{pmatrix} + \begin{pmatrix} N_{hh} & N_{vh} \\ N_{hv} & N_{vv} \end{pmatrix}$$

Or  $\mathbf{M} = A e^{j\phi} \mathbf{R}^T \mathbf{R}_F \mathbf{S} \mathbf{R}_F \mathbf{T} + \mathbf{N}$

- System calibration [Freeman, 2004; Freeman et al., 2008; Shimada et al., 2009]:
  - Calibration without or with Faraday rotation
- Deriving Faraday rotation image using Bickel and Bates' approach [1965]:

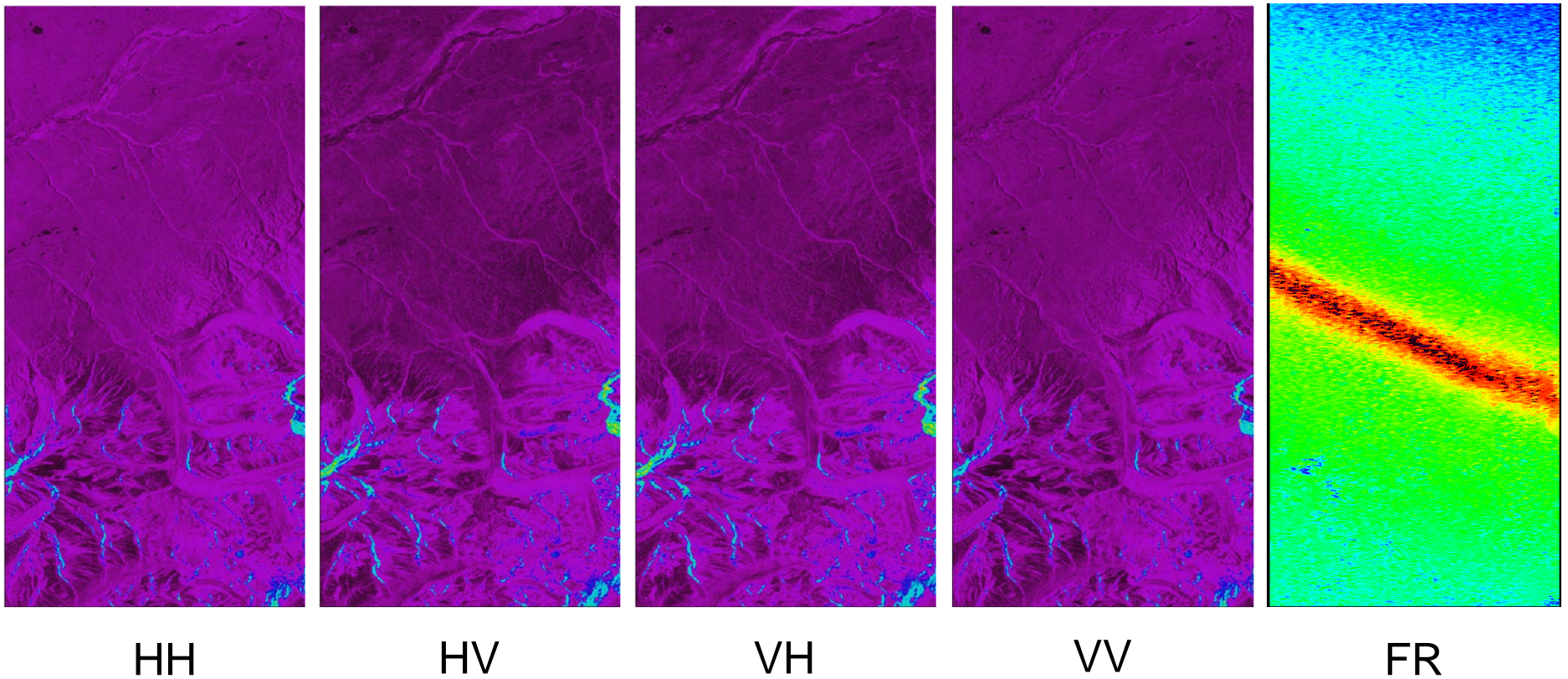
$$\begin{bmatrix} Z_{11} & Z_{12} \\ Z_{21} & Z_{22} \end{bmatrix} = \begin{bmatrix} 1 & j \\ j & 1 \end{bmatrix} \begin{bmatrix} M_{hh} & M_{hv} \\ M_{vh} & M_{vv} \end{bmatrix} \begin{bmatrix} 1 & j \\ j & 1 \end{bmatrix}, \quad \Omega = \frac{1}{4} \arg(Z_{12} Z_{21}^*)$$



# Polarimetric SAR Images

PALSAR Observation

04-01-2007, Alaska: GLAT =  $\sim 62.2^\circ$ , GLON =  $\sim 214.5^\circ$   
during a geomagnetic storm

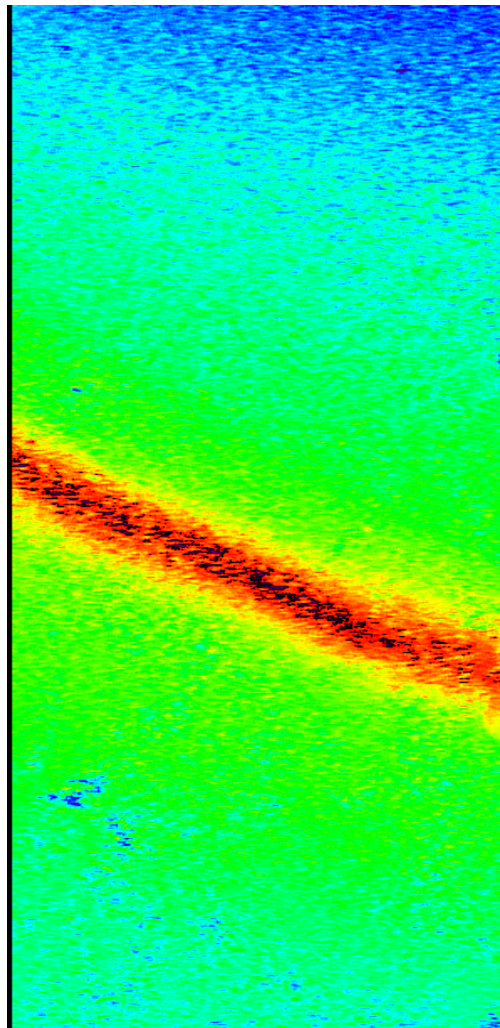


Size of individual images: 18432 x 1248 pixels,  $\sim 66$  km x 29 km.

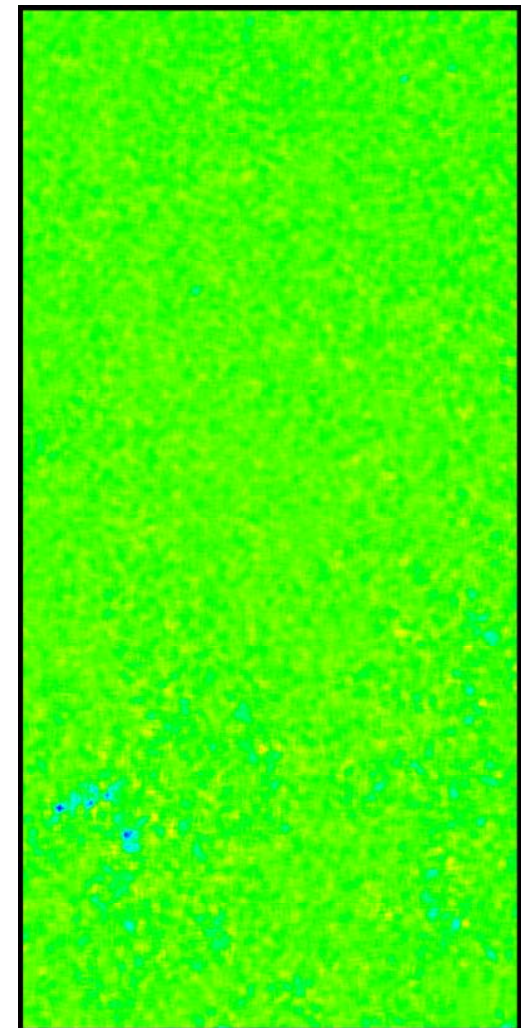


# SAR Polar Ionospheric Images during Storm and Quiet Days

- Faraday rotation images on two days
  - 04-01-2007 (storm)
  - 05-17-2007 (quiet)(repeat orbit, 46 days) when PALSAR illuminated the same area.
- Significant ionospheric difference between the two days.
- The ionospheric arc seen in the 4-1-2007 data is associated with an auroral arc when a geomagnetic storm occurred on 4/1/2007.



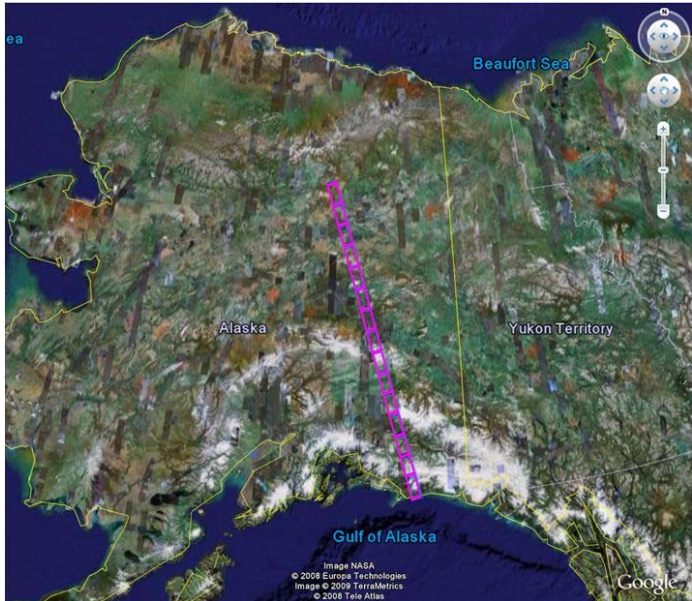
FR



FR

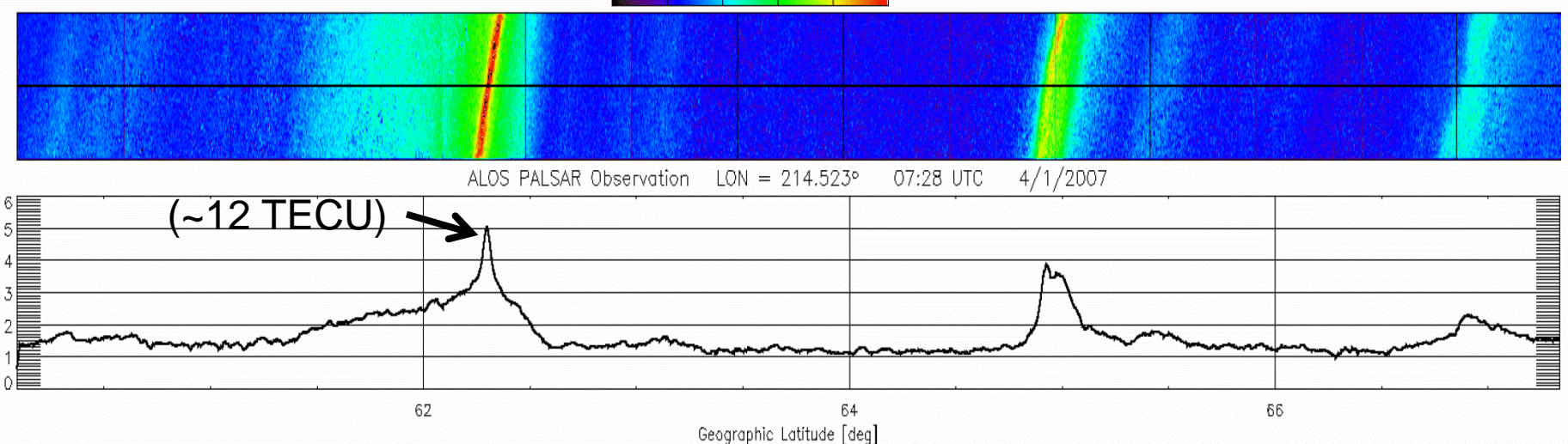


# Polar Ionospheric Arcs Captured in Polarimetric SAR images



- 15 PALSAR image frames are used to compose the Faraday rotation (FR) image strip ( $\sim 900 \times 30 \text{ km}^2$ ).
- Enhanced FR/TEC arcs over the polar region.
- FR structures as small as  $\sim 0.2$  degrees (< 0.5 TECU) are identified after reducing noise.
- Extended enhancements with different gradients surrounding sharp peaks at both edges of the arcs

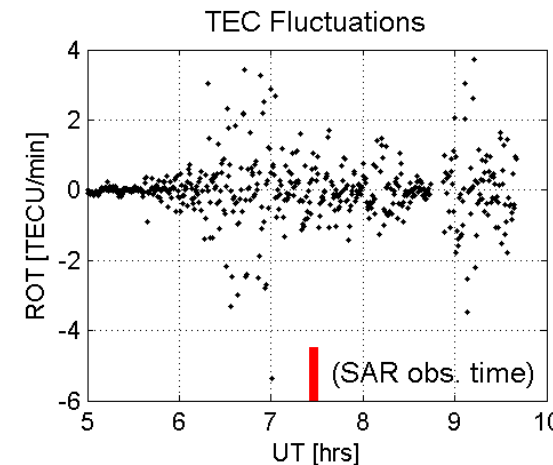
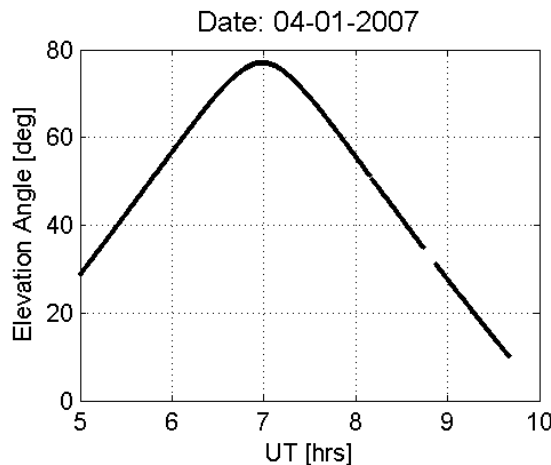
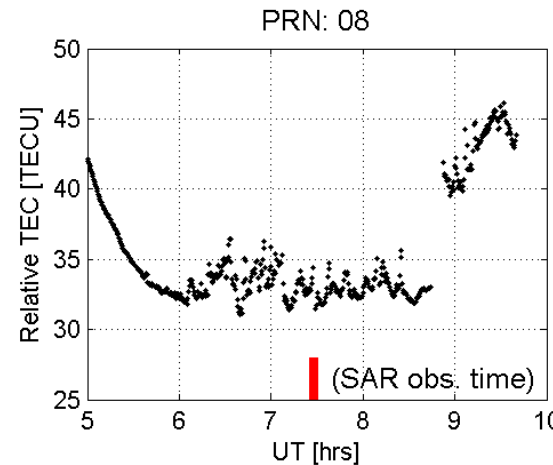
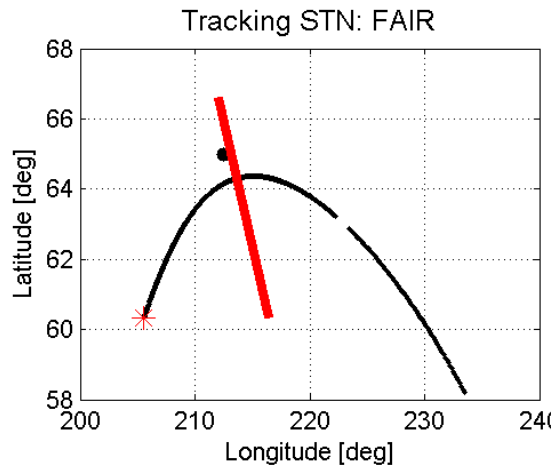
[Pi et al., 2008]





# Ionospheric Irregularities Measured Using GPS in and near the ALOS Path

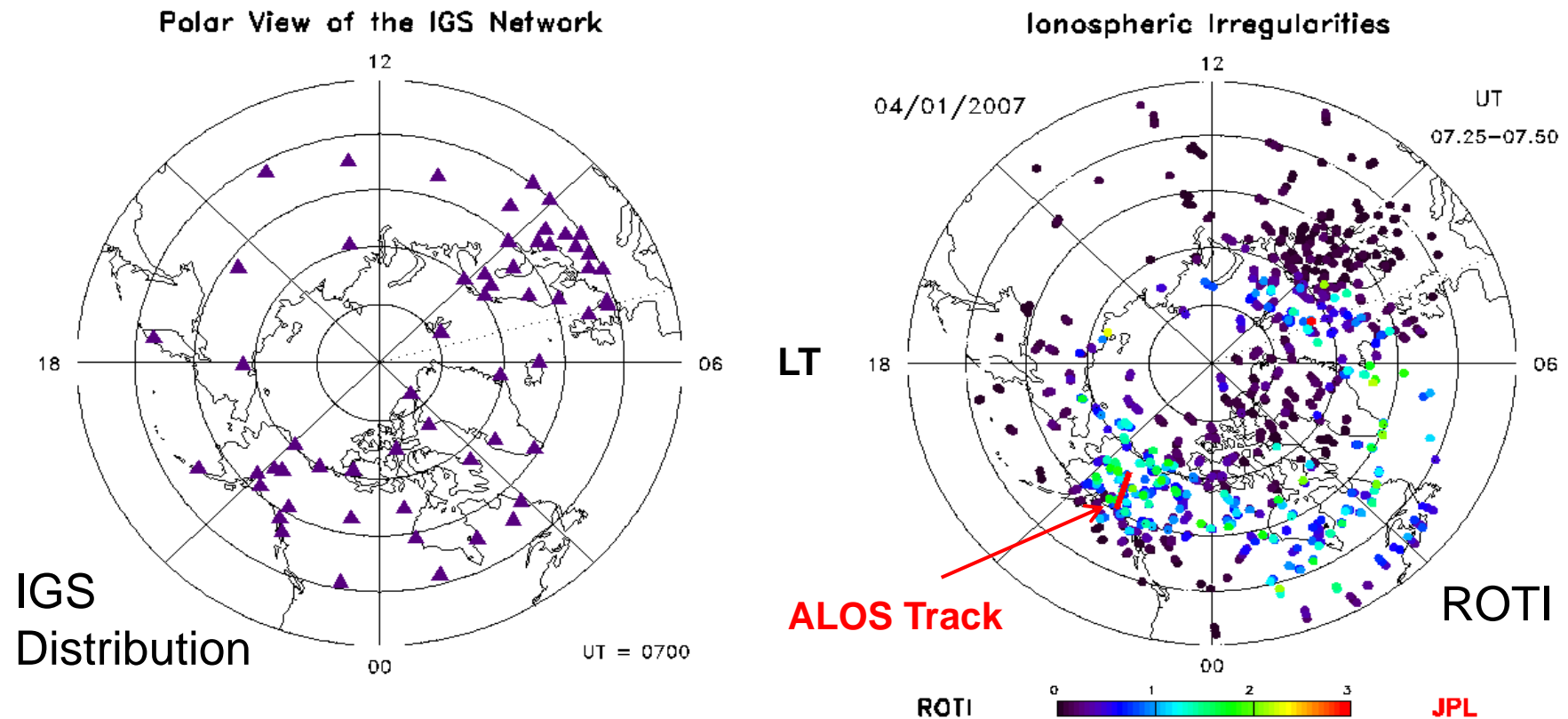
## Red Track: ALOS-PALSAR Path



- Ionospheric irregularities were captured by a GPS receiver at Fairbanks, Alaska, tracking L1 and L2 signals transmitted from PRN-08 satellite.
- At ~07:28 UT, GPS data show TEC perturbations in and near the regions of an ALOS-PALSAR path.



# Snapshot of Ionospheric Irregularities Measured Using GPS

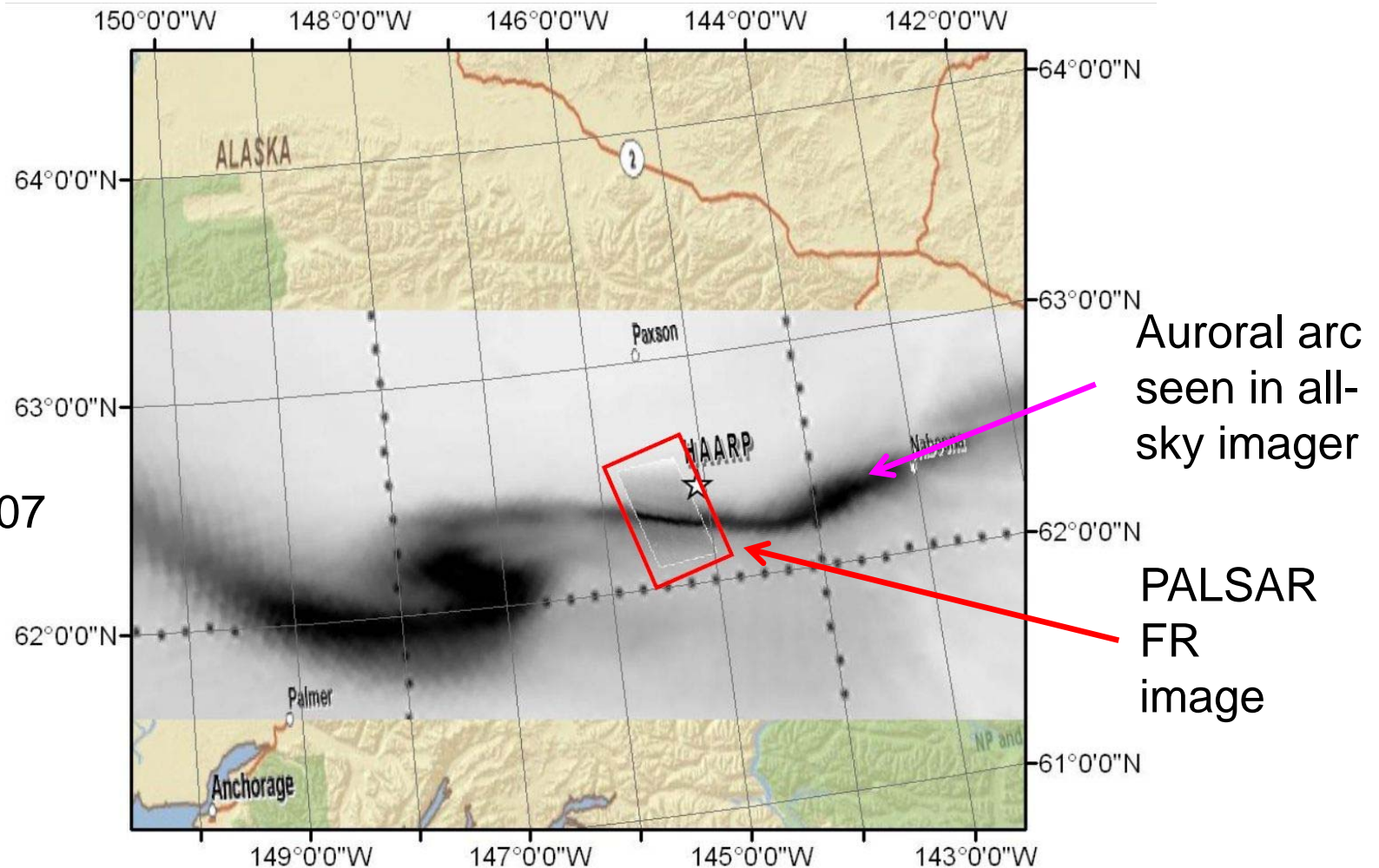


- Dual-frequency GPS observations from 58 stations in the polar region ( $LAT \geq 50^\circ$ ) are processed to produce rate of TEC (ROT) and rate of TEC index (ROTI) measurements
- Increased ROTI values indicate ionospheric irregularities during the storm
- The ALOS-PALSAR passed through a perturbed ionospheric region



# Comparison of SAR and Auroral Images

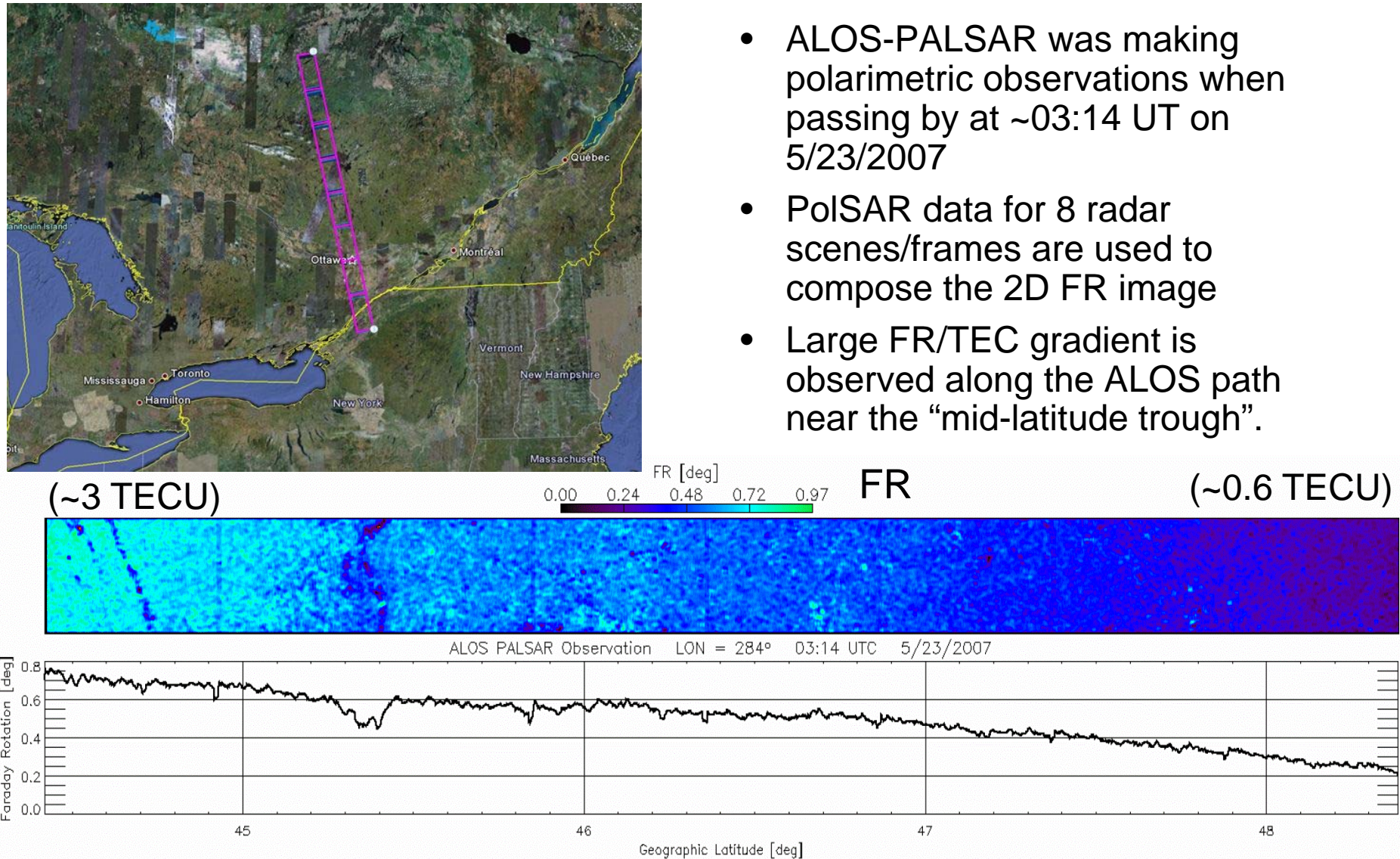
04-01-2007



Comparison between PALSAR and ground-based all-sky auroral images  
[Meyer et al., 2009].

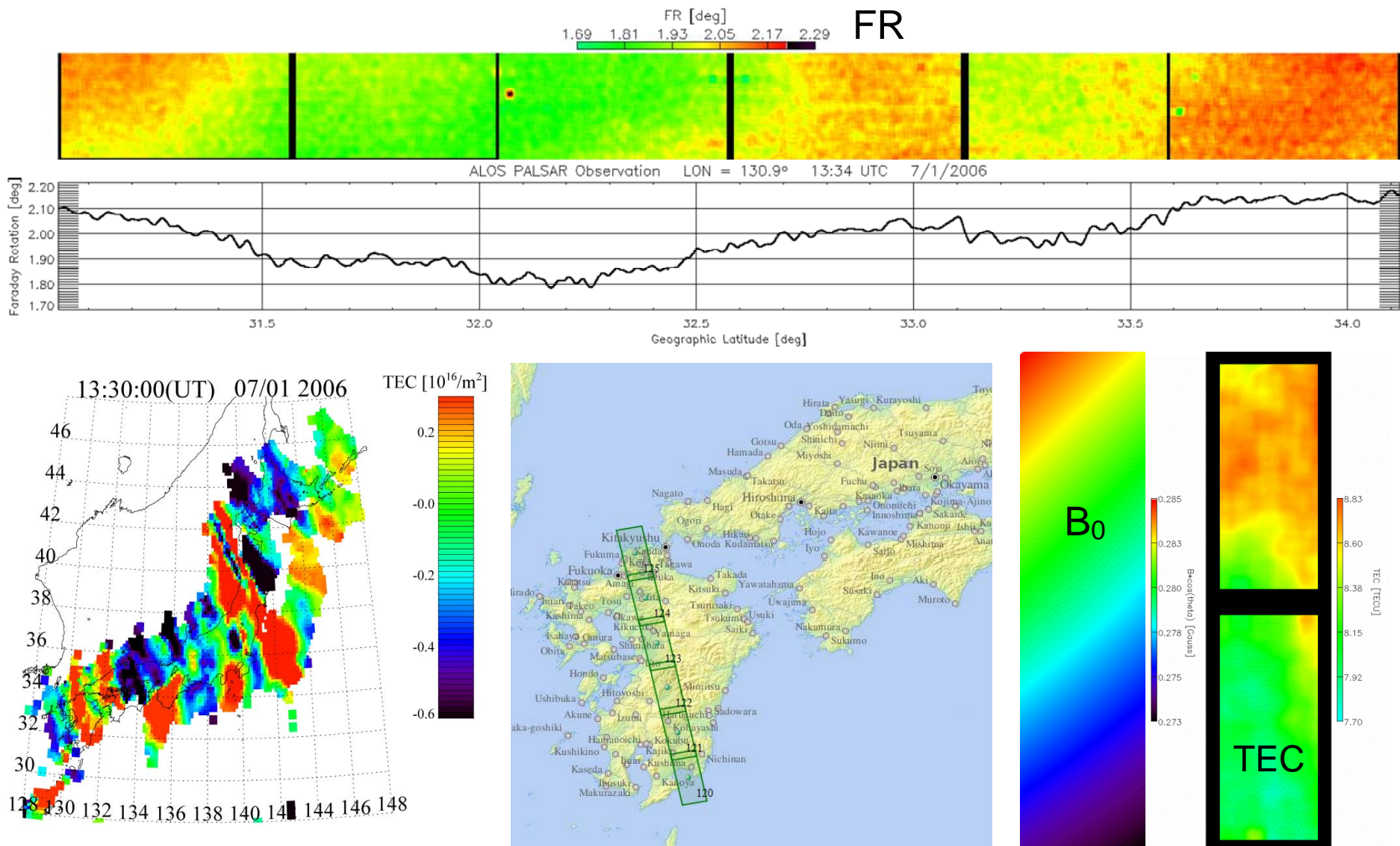


# Mid-Latitude Ionospheric Gradient Captured in PolSAR Images



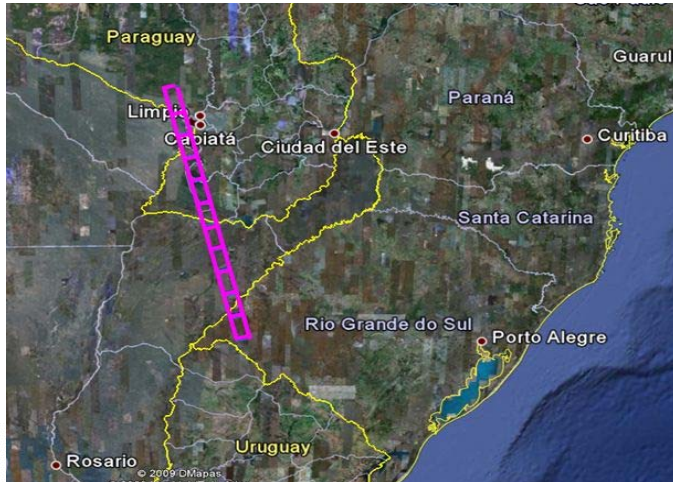


# Imaging TID's at Middle Latitudes



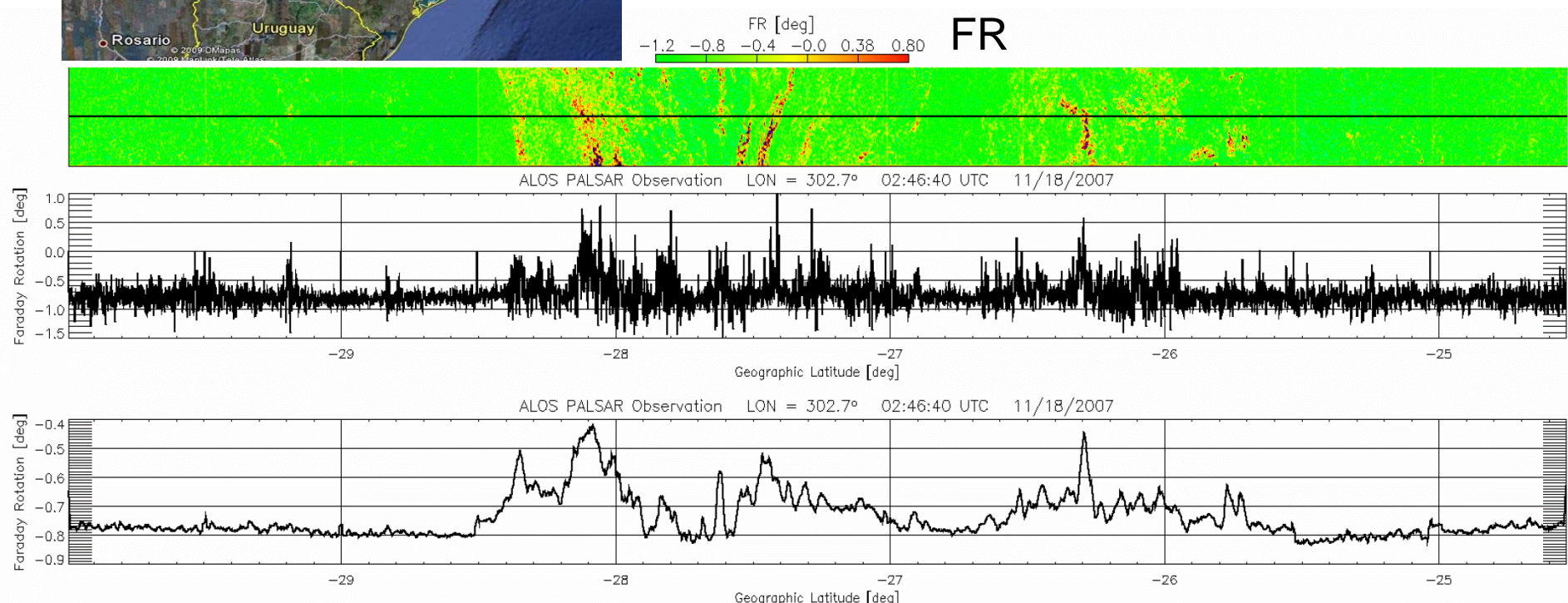


# Ionospheric Scintillation and Plasma Bubbles



Polarimetric observations made using ALOS PALSAR at low latitudes

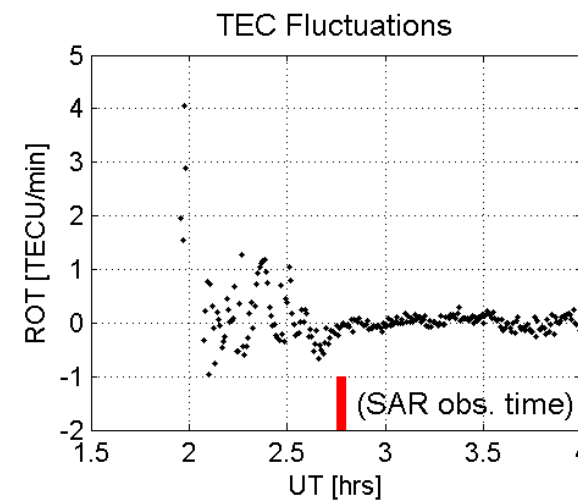
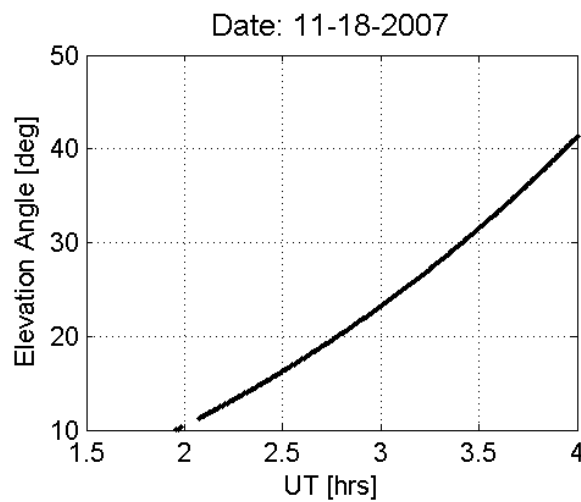
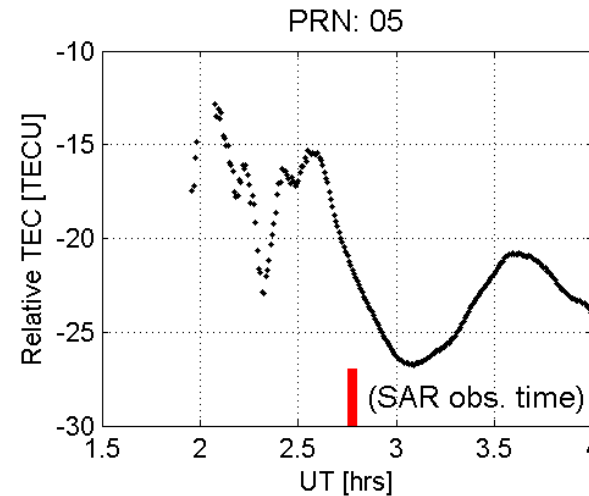
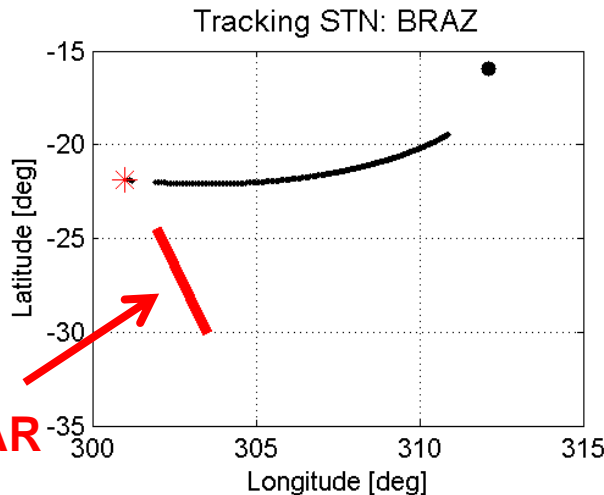
- Faraday rotation scintillation
- Ionospheric depletion/bubbles





# TEC Depletion and Irregularities Measured Using GPS

ALOS-  
PALSAR  
Path

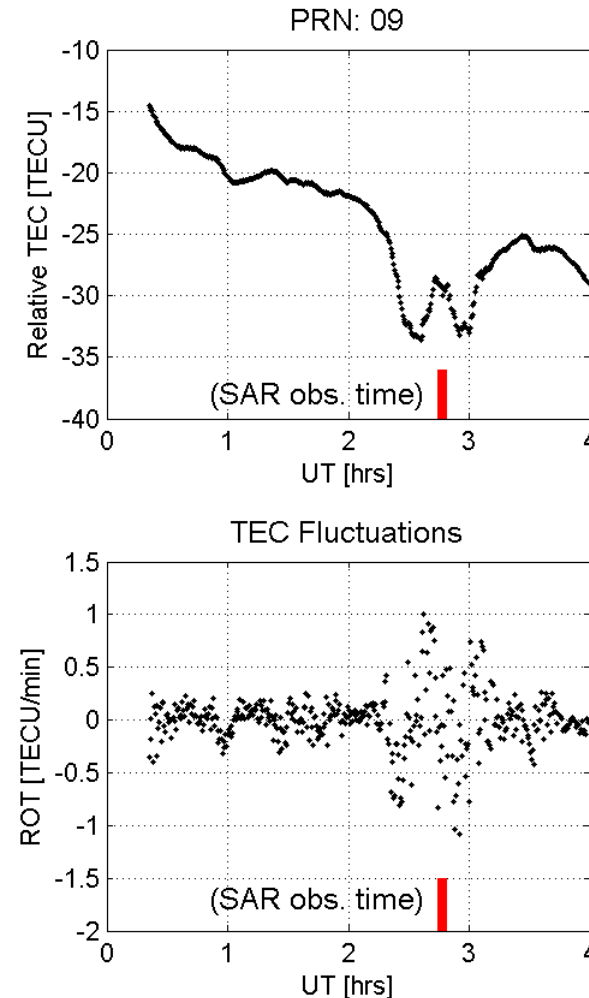
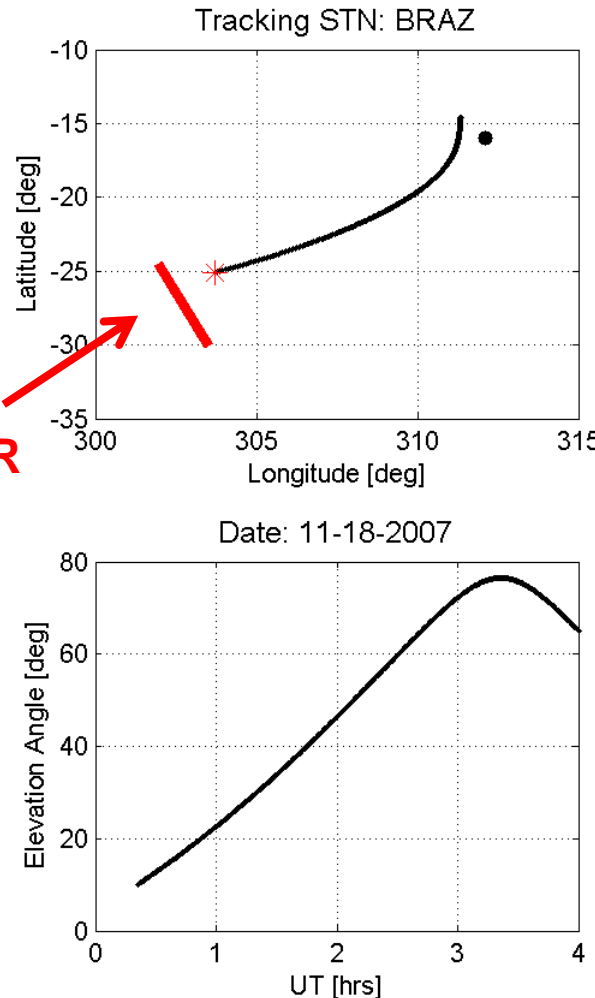


Ionospheric  
Irregularities  
/scintillation  
were  
observed  
in the ALOS-  
PALSAR  
path **before**  
ALOS  
passed by.



# Ionospheric Irregularities Observed Using GPS near a PALSAR Path

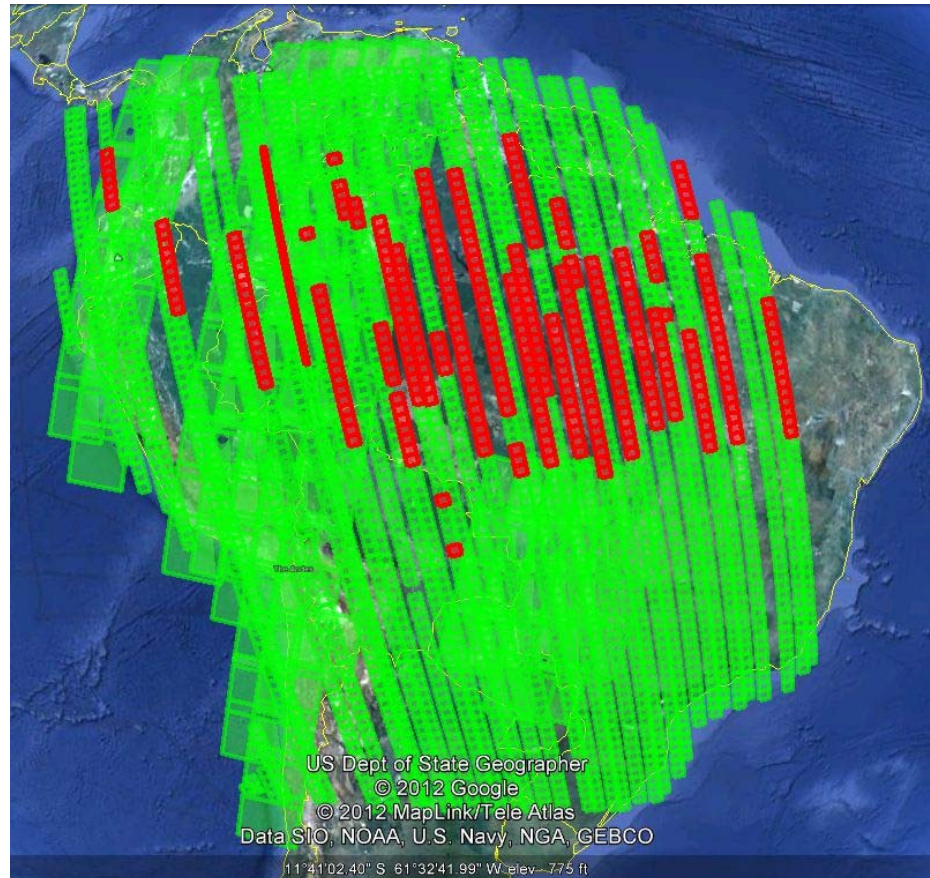
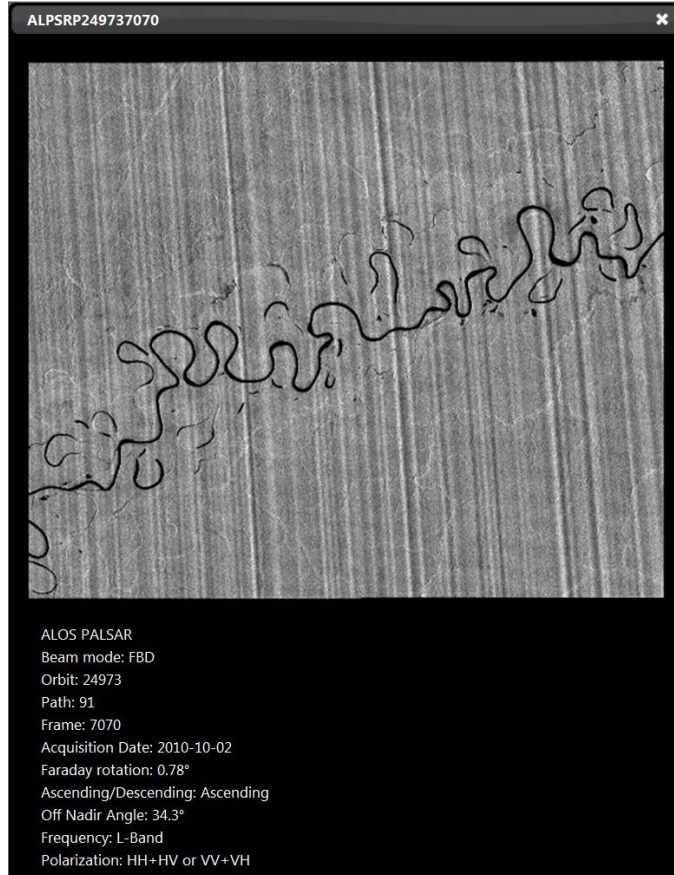
ALOS-  
PALSAR  
Path



Ionospheric  
Irregularities  
/scintillation  
were  
observed  
near the  
ALOS-  
PALSAR  
path when  
ALOS  
passed by.



# Effects of Ionospheric Scintillation



**Example of streaks in PALSAR images  
(effects on ionospheric scintillation)**

A survey of scintillation effects during Oct 2010 (with Meyer and Chotoo):

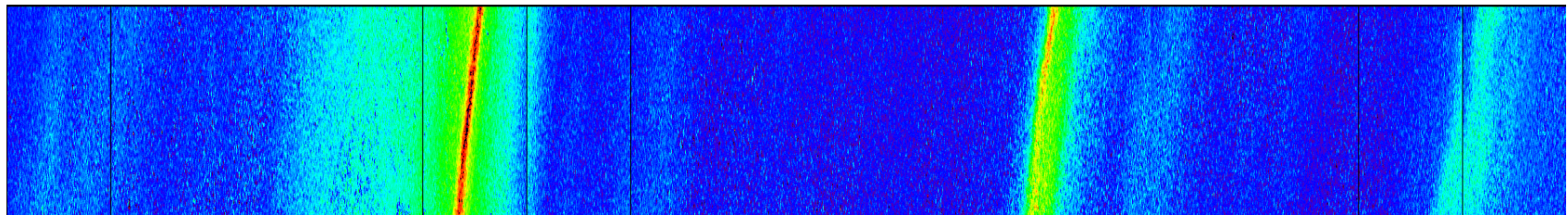
- Total images: 2779
- 14% Images and 74% days affected



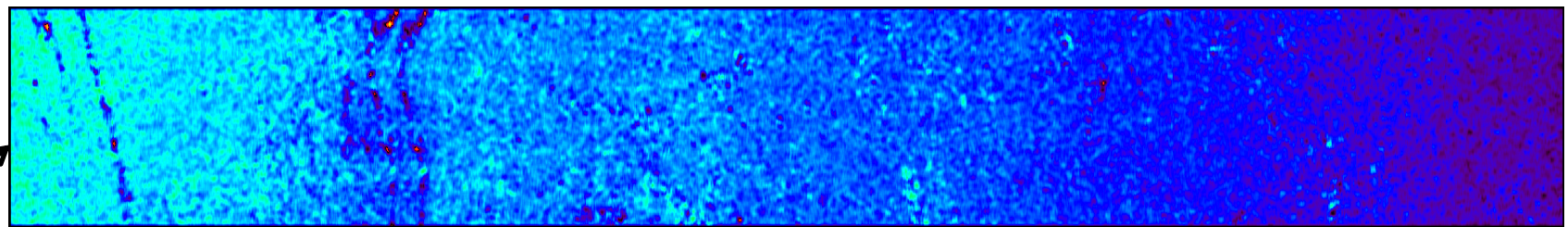
# Summary

## Imaging the Ionosphere Using SAR

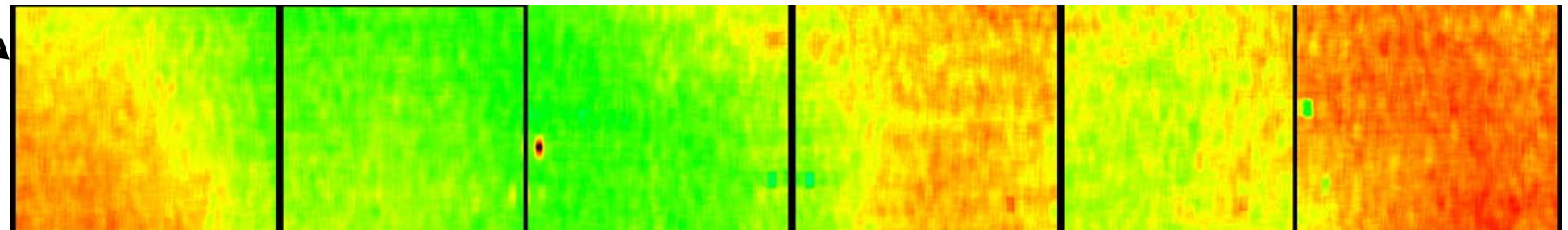
High  
Lat



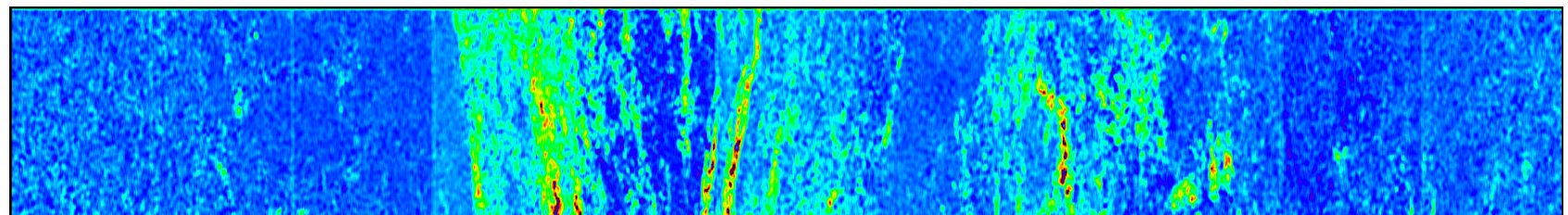
Mid  
Lat



Lat



Low  
Lat



[Images are not in a same scale in → direction.]



# Summary (Cont.)

---

## Advantages

- High resolution: a few hundred meters → ~2 km
- Much less sensitive to weather
  - No concerns about light sources
  - No day/night restriction
- Global coverage
- A new and powerful technique to explore further **ionospheric inhomogeneities and irregularities**
- Will support InSAR and PolSAR ionospheric calibration to ensure **Earth imagery quality** (PolSAR, Split spectrum, etc.)
- Potential to realize lower frequency SAR (P-band)
- A single mission serves both Earth and space sciences

## Limitations

- Very significant data amount with the quad-pol approach
  - requires extraordinary data downlink capacity for continuous operation
- Split-spectral technique can only measure TEC difference under certain conditions
- Limited local time coverage
  - Sun-synchronous orbits
- Relatively low temporal resolution (orbital observations)